Published in final edited form as:
*Clin Neurophysiol*. 2007 November ; 118(11): 2419–2436.

# Individual differences in EEG theta and alpha dynamics during working memory correlate with fMRI responses across subjects

**Jed A. Meltzer**[4], **Michiro Negishi**[1], **Linda C. Mayes**[5], and **R. Todd Constable**[1,2,3,4]

1 *Dept. Diagnostic Radiology, Yale University, New Haven, CT, USA*

2 *Dept. Neurosurgery, Yale University, New Haven, CT, USA*

3 *Dept. Biomedical Engineering, Yale University, New Haven, CT, USA*

4 *Interdepartmental Neuroscience Program, Yale University, New Haven, CT, USA*

5 *Developmental Electrophysiological Laboratory, Yale Child Studies Center, New Haven, CT, USA*

## Abstract

**Objective—**Theta and alpha range EEG oscillations are commonly induced in cognitive tasks, but their possible relationship to the BOLD signal of fMRI is not well understood, and individual variability is high. We explored individual differences in EEG reactivity to determine whether it is positively or negatively correlated with BOLD across subjects.

**Methods—**A Sternberg working memory task with 2, 4, or 6 digits was administered to 18 subjects in separate fMRI and EEG sessions. Memory load dependent theta and alpha reactivity was quantified and used as a regressor to reveal brain areas exhibiting EEG-fMRI correlation across subjects.

**Results—**Theta increases localized to medial prefrontal cortex, and correlated negatively with BOLD in that region and in other "default mode" areas. Alpha modulation localized to parietal-occipital midline cortex and also correlated negatively with BOLD.

**Conclusions—**Individual tendencies to exhibit memory-load dependent oscillations are associated with negative BOLD responses certain brain regions.

**Significance—**Positive BOLD responses and increased EEG oscillations do not necessarily arise in the same regions. Negative BOLD responses may also relate to cognitive activity, as traditionally indexed by increased EEG power in the theta band.

### Keywords

default mode; MEG; deactivation; ERS; negative BOLD

## Introduction

While event-related potentials (ERPs), derived from time-domain averages of EEG signals, have been used for several decades to investigate human cognition, recent years have seen increasing attention paid to other properties of the EEG (or MEG) signal that are also modulated in an event-related manner, but are not precisely phase-locked to the onset of a stimulus, thus

Corresponding Author: Jed A. Meltzer, Yale University School of Medicine, PO Box 208043, TAC N134, New Haven, CT 06520-8043, jed.meltzer@aya.yale.edu, Tel: 203-737-2835 Fax: 203-785-6643.

requiring analysis jointly in the time and frequency domains. Among the most commonly reported phenomena are event-related synchronization (power increase) and desynchronization (power decrease) in distinct frequency bands, including theta (~ 4–7 Hz), alpha (~ 8–12 Hz), beta (~ 15–25 Hz), and gamma (> 30 Hz). The theta frequency range has been of particular interest in cognitive neuroscience, due to its proposed homology with rodent hippocampal theta rhythm (Bastiaansen and Hagoort, 2003, Miller, 1991) and the fact that it is commonly observed to exhibit power increases associated with greater levels of mental effort or cognitive challenge (Gevins, 1979, 1997, Gundel and Wilson, 1992, Inanaga, 1998). Task contrasts that elicit theta increases have included successful vs. unsuccessful memory encoding (Sederberg et al., 2003, Klimesch et al., 1996) and retrieval (Burgess and Gruzelier, 2000, Guderian and Duzel, 2005), working memory load (Gevins et al., 1997), and sentence processing (Bastiaansen et al., 2002a), to list only a few examples.

In contrast to the theta band, power in the alpha band is often seen to decrease under conditions of greater demand, primarily at posterior sites, (Gevins et al., 1979, 1997, Vanni et al., 1997, Gundel and Wilson, 1992), although numerous exceptions have been reported, in which cognitive tasks elicit increases in alpha power (Schack and Klimesch, 2002, Klimesch et al., 1999, Bastiaansen et al., 2002b). Nonetheless, event-related desynchronization of the alpha band is an extremely common finding, leading to proposals that alpha oscillations can represent an “idling” state of cortex (Van Winsum et al., 1984, Miller, 2007). Therefore, increases in frontal midline theta (henceforth, “Fm theta”) and decreases in posterior alpha together represent a general profile of EEG effects for increasing levels of cognitive demand in a variety of language and memory tasks. Given the ubiquity of such findings, there is much interest in understanding the relationship between EEG oscillations and the BOLD signal measured in fMRI, which provides another quantitative measure related to neuronal information processing, with great spatial specificity. General spatial dissociations in fMRI signal changes across a variety of tasks have also been reported, such that increases in memory and attentional demands are often observed to elicit negative signal changes in a set of regions dubbed the “default mode network” (Raichle et al., 2001), which includes frontal and parietal-occipital midline regions along with the bilateral angular gyri. Similarly, positive signal changes are commonly observed in bilateral prefrontal and parietal areas (Fox et al., 2005, Fransson, 2006), which have recently been called a “task-positive” network. As yet, it is an open question whether event-related changes in theta and alpha power are generated in the same regions exhibiting BOLD effects in cognitive tasks, and whether the correlation between task-modulated EEG power and BOLD is positive or negative in specific regions and frequency bands.

While numerous studies have employed simultaneous EEG and fMRI measurements, they have generally not investigated event-related power changes. Rather, they have generally examined spontaneous power fluctuations occurring during long blocks of rest or mental arithmetic. Several studies of the resting state have shown a negative correlation between alpha power and BOLD in cortex (Goldman et al., 2002, Moosmann et al., 2003, Laufs et al., 2003), consistent with an “idling” role, although considerable individual variability is also present (Laufs et al., 2006), including instances of positive correlations (Goncalves et al., 2006). To date, two EEG-fMRI studies of the theta band have employed mental arithmetic, which is known to elicit theta increases in some subjects (Inanaga, 1990, Miwakeichi et al., 2004), but have reached somewhat different conclusions. Mizuhara et al. (2004) found negative correlations between theta power and BOLD in anterior medial cortex, in close correspondence with the putative sources of frontal theta as estimated in MEG studies (Asada et al., 1999, Ishii et al., 1999), while positive and negative correlations were also observed in distant areas, suggesting that theta reflects metabolic deactivation in the cortex that generates it, while other areas may be anticorrelated with such activity. In contrast, Sammer et al. (2006) used a very similar paradigm, but reported exclusively positive correlations with fluctuations in theta power, in widely-distributed regions of the brain.

While simultaneous EEG-fMRI studies have yielded important insights into the relationship between the two modalities, they do have some limitations. For instance, it is well known that brain regions comprising the afore-mentioned task-positive and default mode networks exhibit highly correlated spontaneous fluctuations within each network (Fransson, 2006), and anticorrelated activity between the networks (Fox et al., 2005). Even if the observed EEG phenomena were generated in only one node of the network, they could be expected to exhibit correlations with many different brain regions. Therefore, other methods have also been employed to investigate E/MEG-fMRI relationships, including direct comparisons of BOLD with MEG source estimates (Brookes et al., 2005) and intracranial recordings obtained from neurosurgery patients (Mukamel et al., 2005, Lachaux et al., 2007) and from animals (Logothetis et al., 2001, Niessing et al., 2005). In the present study, we use a novel method for the exploration of EEG-fMRI relationships: the exploitation of inter-subject variability.

Inter-subject variability is particularly high for Fm theta, and has been commented on since the earliest reports of theta oscillations in human EEG (for review, see Inanaga, 1998). Given this high variability, some studies of theta power reactivity have resorted to prescreening human subjects for the presence of theta responses prior to conducting the main experiment (e.g. Miwakeichi et al., 2004). Since subjects vary in the degree to which (or whether at all) they exhibit Fm theta increases to increasing cognitive demands, the examination of correlations across subjects between EEG and fMRI responses offers another window on the potential relationship between these two modalities. Therefore, we sought to develop a task with parametrically modulated levels of cognitive demand that was well suited for measurement in both EEG and fMRI. We chose the Sternberg working memory task. In this task (Sternberg, 1966), a subject is required to remember a set of items during a delay period, in order to identify a probe item as present or absent from a memorized list. The number of items in the set can vary across trials, allowing the assessment of signal changes that are parametrically related to working memory load. This task has been used extensively in fMRI, demonstrating load-dependent increases in the BOLD signal in frontal areas such as the middle, superior, and inferior frontal gyri, the precentral gyrus, and also in parietal and cerebellar regions (Rypma et al., 1999, Jha and McCarthy, 2000, Narayanan et al., 2005, Zarahn et al., 2004, Kirschen et al., 2005), while load-dependent decreases have been reported less often (c.f. Habeck et al., 2005).

An attractive feature of the Sternberg task is that memory load effects that are highly variable across subjects have already been reported in EEG/MEG studies. In an MEG study, Jensen and Tesche (2002) found that power in the 7–8.5 Hz range increased significantly with greater memory load during the delay period of the Sternberg task. However, in a complementary EEG study, Jensen et al. (2002) did not replicate the MEG findings, but instead found that power in the alpha range (8–12 Hz.) at posterior electrodes was significantly increased with load. Nonetheless, a frontal theta power increase was apparent in the group average data, but this increase was driven almost entirely by one subject out of ten, who had an extremely large theta response. In a subsequent study, Onton et al. (2005) analyzed the trial-by-trial variability of theta responses in the Sternberg task, finding that even statistically significant load-modulated increases in theta power in individual subjects can be driven by a subset of extremely reactive trials, while other trials show very little response.

In the present study, we have attempted to capitalize on the high inter-subject variability of EEG oscillations during the Sternberg task, in order to elucidate the relationship between low-frequency EEG activity (theta and alpha bands) and the memory load-dependent BOLD signal changes commonly observed in this task. We devised a version of the Sternberg task suitable for both fMRI and EEG measurements, and collected data from both modalities in separate sessions on 18 subjects. The outcome of the EEG measurement was used as an independent variable, testing whether inter-subject differences in EEG reactivity predict patterns of fMRI

signal changes. The detection of significant correlations across subjects between scalp EEG and fMRI reactivity, combined with direct source localization estimates of EEG activity, can help to determine where in the brain the EEG activity is generated, and whether it is positively or negatively correlated with the BOLD signal.

# METHODS

## Subjects

18 participants were recruited from the Yale University Community, ranging from 23 to 35 years old (mean age 27, 10 females). All subjects gave informed consent, had normal or corrected vision, and were paid for their participation. The study protocol was approved by the Yale University Human Investigation Committee. All subjects completed the fMRI session first, and the EEG session second. For thirteen subjects, the fMRI and EEG sessions were conducted three days apart from each other, while the intersession interval varied up to three weeks for the other five subjects. Because the primary goal of this study was to examine intersubject differences, we did not counterbalance the order of sessions across subjects, as it would have introduced a confound. The fact that a practice effect may be present in the EEG session (see results) does not confound the main findings of the experiment, which relate to correlations across subjects between fMRI and EEG reactivity.

## Sternberg Task

At the onset of each trial, a stimulus array of six items, arranged in two rows, appeared in black font at the center of a constant white background (fig. 1A). On trials with the highest memory load, each item of the array was a digit, selected randomly without replacement from 0 to 9. On trials with lower memory loads, two or four of the items were digits, and the remaining items were plus signs. The locations of the digits within the array were random. The plus signs were used as fillers to ensure that the total amount of purely visual stimulation was approximately constant across trials. While both digits and letters have proven effective at inducing the typical memory load-dependent reaction time increment in the Sternberg task (e.g. Sternberg, 1966,Zarahn et al., 2005), we chose to use digits, in order to encourage a more uniform strategy of rote mental rehearsal, rather than the use of mnemonic associations. However, subjects were not explicitly instructed requested to use any particular strategy, but simply to “remember” the digits during the delay period. The stimulus array remained on the screen for 3.1 seconds, after which it was replaced by an array of three dots, intended to minimize confusion between the delay period and the inter-trial interval, during which only a blank screen was presented. After a 10.85-second delay period, a single probe digit appeared at the center, with question marks on either side of it. Subjects were to press the left button of a fiber-optic response box if the probe digit was among the stimulus array for that trial (“yes” responses) and the right button otherwise (“no” responses). The probe digit was displayed for 1.55 seconds, and subjects had a time limit of 3.1 seconds to respond to it. The inter-trial interval varied randomly from 3.1 to 7.75 seconds, in integer multiples of the MR pulse sequence repetition time (TR=1.55 seconds). The task was exactly the same for the fMRI session and the EEG session, except for the differences between the fMRI and EEG recording environments, and the use of unique stimuli for each session. Each run comprised 18 trials, 6 of each condition, and lasted a total of 4 minutes, 39 seconds. Subjects completed 7 runs in the fMRI session, and 7–9 runs in the EEG session, depending on time available.

## FMRI acquisition

FMRI was performed on a 3-Tesla Siemens Trio system. Foam padding and tape were used to minimize head movement. Stimuli were projected onto a mirror mounted on the head coil above the subject’s face. Subjects’ responses were registered using a fiber-optic button box (Current Designs, Philadelphia, PA) and scanning noise was muffled through the use of earplugs and

passive sound-blocking MRI-compatible headphones (Resonance Technologies, Northridge, CA). After localizer scans, 25 axial slices were defined covering the whole brain, parallel to the line between the anterior and posterior commisures. In this orientation, we first acquired a T1-weighted anatomic image. Next, subjects performed the cognitive task during acquisition of functional EPI images (64×64 matrix, FOV 220 mm, TE 30 ms, TR 1550 ms, in-plane voxel size 3.4×3.4 mm, slice thickness 6mm, no skip, interleaved ascending acquisition, $\alpha = 80°$), in the same AC-PC aligned 25-slice geometry. Seven runs of 18 trials each were performed. After completion of the cognitive task, a high-resolution 3D MPRAGE anatomical image was acquired.

## FMRI analysis

FMRI preprocessing and statistical analysis were conducted with AFNI software (http://afni.nimh.nih.gov/afni/), supplemented by programs written locally in MATLAB 6.5 (Mathworks, Natick, MA). EPI images were skull-stripped (Brain Extraction Tool, http://www.fmrib.ox.ac.uk/fsl/), corrected for differences in slice-timing, motion-corrected, smoothed with a 8mm FWHM kernel, and normalized so that the mean of every voxel's timecourse in each run was 100, allowing subsequent regression parameter estimates to be interpretable as percent signal change. For the primary statistical analyses of the fMRI time series, we used a standard hemodynamic response model in the form of a gamma density function with default parameters (Cohen, 1997). The timing of each trial, consisting of two TRs of encoding, 7 TRs of delay, and 1 TR of retrieval, was convolved with that function, and regression parameters were estimated for encoding, delay, and retrieval for each condition. As the average reaction time in all conditions was less than the length of one TR, the probe retrieval event was modeled as one TR, rather than the entire 2-TR period during which the probe digit was displayed. In addition to the primary model-based analysis, we also employed deconvolution techniques (Miezin et al., 2000) in order to estimate the condition-specific impulse response function (IRF) at 15 timepoints, ranging from 0 to 21.7 seconds relative to the onset of the encoding period. This second analysis was used primarily for display purposes, allowing for the visualization of the BOLD timecourses in specific regions identified in the multi-subject statistical analyses, separately averaged in each condition (2, 4, or 6 digits). Furthermore, the empirical estimation of the IRF provided confirmation that the data were appropriately modeled as the convolution of standard hemodynamic response functions with the three phases of each trial.

Functional images resulting from within-subject statistical analysis were warped into a reference space (the "Colin brain," http://www.mrc-cbu.cam.ac.uk, skull-stripped locally) with MNI coordinates, using a three-step transformation: a 6-parameter rigid transformation from the EPI image to the axial anatomical, a 6-parameter rigid transformation from the axial anatomical to the high-resolution MPRAGE image, and a 12-parameter affine plus nonlinear grid-based transform (Papademetris et al., 2004) from the individual subject's skull-stripped MPRAGE to the reference brain, implemented with in-house software. For all multi-subject tests, percent-signal change values for each subject were submitted to statistical analyses, thus treating subjects as a random effect (Friston et al., 1999). To correct for multiple comparisons across voxels, a minimum cluster size threshold was adopted (Forman et al., 1995). Using a voxel-wise threshold of $p<.01$, Monte Carlo simulations (the AFNI program *Alphasim*) were used to set a cluster size criterion of 2.16 mL (279 voxels), in order to control the family wise error rate at $p<.05$.

## Estimation of memory load effects

The primary goal of this experiment was to assess across-subject correlations between EEG and fMRI reactivity to increasing levels of working memory load. Three levels of memory load were chosen in order to confirm that increased activity is indeed parametrically modulated by

load (precluding the use of only 2 levels), while allowing for a reasonably large number of trials in each condition (precluding the use of many different levels). In order to assess between-modality correlations in a parsimonious manner, we employed a single contrast testing for a linear effect of load across the three experimental levels (2, 4, and 6 digits). A single parameter estimate for load effects in the encoding period, and another one for the delay period, were thus generated for each subject, to be submitted to the second-level random-effects analyses across subjects. Notably, in the case of a linear trend analysis with three equally spaced levels, the magnitude of the estimated load effect for each subject is exactly equivalent to the simple subtraction between the two extreme levels (here, 6-digit minus 2-digit), except for an optional scaling factor. Therefore, we chose to use this subtraction as the primary measure of interest, which is perfectly adequate as long as load modulation is approximately linear. However, the presence of a "U-shape curve" in the response to increasing levels of memory load could invalidate the use of a single contrast. In order to check for such an effect, we compared the results of two different group-level analyses. In the first analysis, we simply submitted the load-effect contrast calculated for each subject (6-digit minus 2-digit) to a one-sample t-test. We also computed equivalent maps for the other pairwise comparisons 6–4 and 4–2. In the second analysis, we submitted the delay period regression coefficients from each condition (2,4, and 6 digits) to a voxel-wise repeated measures 1-factor ANOVA, testing for a main effect of memory load, irrespective of the linear ordering of the three levels. The output of the ANOVA was examined in order to determine whether any nonlinear effects of different memory load levels (e.g. a U-shaped curve) were present in the fMRI data.

### EEG recording and preprocessing

The design of the present experiment, as a multimodal paradigm suitable for both fMRI and EEG, required the use of specialized procedures for EEG processing. Normally, EEG experiments comprise individual trials that are fairly short in length. For instance, a retention interval of 2–3 seconds is typical in working memory experiments (e.g. Jensen et al., 2002, Schack et al., 2002). The use of a large number of short trials allows for an easy way of dealing with EEG artifacts such as blinks: simply discard trials that contain artifacts. In fMRI studies of working memory, much longer delay periods are employed, due to the necessity of identifying lagged hemodynamic activity attributable to the delay period of the task, as opposed to the encoding period. In this experiment, the total length of each trial was 17.05 seconds, meaning that almost every trial contained blinks, along with other artifacts. Rather than excluding whole trials, therefore, we employed Independent Component Analysis (ICA) to remove signals attributable to artifacts, while retaining signals attributable to brain electrical activity. Briefly stated, the EEG signal at each sensor site was reconstructed from a subset of independent components (ICs), and these reconstructed signals at each sensor site were used for multi-subject analysis. We did not conduct any multi-subject analyses on ICs directly. However, in addition to artifact removal, ICs were used for display purposes. In order to illustrate examples of oscillatory activity strongly modulated by memory load within individual subjects, we displayed the results of spectral analysis on single components exhibiting the effects, rather than selecting an arbitrary channel to display (see results). In these cases, the scalp map showing the spatial projection of each IC provides an indication of the spatial extent of the load-modulated activity.

125-channel EEG was recorded with a Geodesic Sensor Net (EGI, Eugene, OR), sampled at 250 Hz with a hardware bandwidth of 0.1–100 Hz, initially referenced to site CZ (later converted to average reference, see below), and bandpass filtered (0.5–30 Hz) offline. Data were exported to EEGLAB software (Delorme and Makeig, 2004) for analysis. Five consecutive nonoverlapping 1.8-second epochs were extracted from the middle of the delay period of each trial of the Sternberg task, during which time the subject was rehearsing the digits and no externally-driven events occurred. Thus, brief periods (.925 seconds) at the

beginning and end of the delay period were not included. The 1.8 second epoch length was chosen as a convenient length for rejecting individual epochs and carrying out spectral analysis (see below). The use of the entire delay period as a single epoch would necessitate the discarding of more data, and would result in fewer epochs being averaged in spectral estimates, thus reducing the reliability of those estimates. The 1.8-second epochs were manually screened for severe artifacts, and badly contaminated epochs (<5%) were discarded. In some cases, individual channels judged to be highly contaminated by artifact were also excluded. Decisions about rejecting individual epochs, channels, and ICs were made by an experimenter conducting visual inspection, blind to which condition the epochs belonged to. Arbitrary amplitude thresholds for artifact rejection were not used.

Epochs were then submitted to InfoMax ICA (Delorme and Makeig, 2004). Following the suggestions of the EEGLAB tutorial material (http://www.sccn.ucsd.edu/eeglab), two rounds of ICA were used to remove artifacts and reduce the dimensionality of the data, as the results of the initial round are informative in rejecting more epochs. First, PCA was employed to reduce the 125-channel data to 80 dimensions, which were then decomposed into 80 ICs. Component scalp maps, timecourses, and spectra were visually examined to identify components dominated by artifacts, which were selected for rejection. Additionally, individual epochs during which most ICA components had abnormally high amplitude were identified as artifactual (likely due to subject movement, also <5%) and removed. Criteria for IC rejection included correspondence to known artifacts such as heartbeat and eye movement (defined by waveform appearance, spatial projection patterns, and power spectra, collapsed across all conditions so that the hypotheses of the experiment would not bias component selection), spatial projection to only one channel, or high amplitude during only a small portion of the total experimental time. Most components met one or more of these criteria and were rejected. The majority of the 80 components in each subject projected only to one channel at a few moments in time, and accounted for very little of the total variance in the data, representing noise specific to a single electrode. Next, the EEG signals at individual channels were reconstructed by multiplying only the non-rejected ICs by their spatial projections. Then, the reconstructed data were converted to an average-reference montage. This step was carried out after ICA so that eyeblink activity would not contribute to estimates of the average voltage. The resulting EEG data was then submitted to a second round of ICA, and more artifactual epochs and components were removed, using the criteria described above. A range of 8 to 22 components (mean = 15) were retained for each subject, comparable to results reported in other studies employing these methods (Onton et al., 2005). Next, the whole sequence of ICA decompositions, component subtractions, and average referencing (using the weights computed from the 1.8 second epochs extracted from the delay period) was applied to the entire EEG dataset, consisting of from 126 to 162 whole-trial epochs per subject. This resulted in a dataset of full-length trials, reconstructed from the 8–22 ICs retained in each subject. These whole-trial epochs extended from 2 seconds prior to digit onset to 17 seconds after, just before the offset of the probe digit at the end of the trial.

## EEG spectral analysis

The primary variable of interest in the EEG data was the effect of memory load on spectral power during the encoding and delay periods, which was to be compared with fMRI load effects across subjects. To estimate spectral power during these periods, we employed multi-taper spectral analysis (Percival and Walden, 1993) on individual epochs for each electrode, and then averaged the resulting power spectra within each condition. For spectral analysis of delay period activity, we used the same 1.8 second epochs described above. For the encoding period, we extracted data from the reconstructed whole-trial epochs, in a time range of 0.1 to 3 seconds after the appearance of the digit array. Because the absolute amplitude of EEG oscillations is dependent on skull conductivity and geometry as much as it is on neuronal dynamics, average

spectra were normalized by dividing by the total amount of power from 0.5–30 Hz, averaged across all conditions, prior to computing relative change scores for submission to multisubject averaging and EEG-fMRI correlation analysis. This normalization is also desirable because memory load effects in fMRI are routinely normalized to percent signal change. Spectral analysis was also performed on the retained ICs for each subject, to identify components strongly modulated by memory load.

Spectral analysis of whole epochs with the multi-taper method provides a good estimate of the average level of power in different frequency bands during the epochs, but does not provide an estimate of the specific timecourse of power throughout the trial. Therefore, we also conducted a time-frequency analysis using the Event-Related Spectral Perturbation method ("ERSP", Makeig, 1993), implemented in EEGLAB. As this analysis was conducted for display purposes, not for multi-subject analyses, we conducted it only on the retained ICs, and not on the individual channels. A sliding window FFT spectrogram was computed on each whole-trial epoch (300 Hanning windows, window length 4.1 sec, 99% overlap), which was then log-transformed. The log-transformed average power spectrum from the pre-stimulus baseline period was subtracted from each segment's value, yielding the ERSP. ERSP values were averaged separately in each condition. ERSP values were averaged across prespecified frequency ranges in the theta (4–7 Hz) and alpha (8–12 Hz) bands in order to generate plots of the timecourses of spectral power evolution throughout the trial. Theta was defined as 4–7 Hz to minimize overlap with the alpha band, especially in subjects with a lower alpha peak frequency.

## EEG-fMRI correlation analysis

In order to determine whether individual variability in EEG reactivity to increased memory load was related to variability in BOLD responses, we computed the Spearman's rank-order correlation coefficient ("rho") between the BOLD load effect and the EEG load effects. Four comparisons were possible: theta and alpha bands, in encoding and delay periods. However, as high inter-subject variability was observed in EEG only in the delay period, we did not expect, and did not detect, any significant correlations for the encoding period. Each subject contributed one fMRI value at each voxel, representing the difference between the BOLD regression coefficients for 6-digit versus 2-digit trials.

As explained above, this quantity is the best single estimate of the linear load effect for each subject – identical results are obtained from a linear regression performed within each subject. For the EEG data, a single region of interest was defined in order to compute a single subject-specific estimate of the load modulation effect in each frequency band of interest. EEG ROIs were not precisely defined *a priori*, but selected on the basis of the group averaged EEG results considered independently of the fMRI data. We selected regions of maximum reactivity in the group averages, regardless of whether that reactivity was statistically significant across the whole cohort. As these regions were defined purely on the basis of EEG reactivity independent of fMRI results, the *a posteriori* definition of EEG ROIs does not bias the observed inter-modal correlations.

As expected, maximum theta reactivity was observed in a frontal midline region, while maximum alpha reactivity occurred in a parietal-occipital region straddling the midline (see results). The load effect for each subject (again, defined as the 6–2 subtraction) was calculated at each electrode by subtracting the averaged spectral power across the theta (4–7 Hz) and alpha (8–12 Hz) bands. The resulting difference values were then averaged across the electrodes that comprised the EEG ROI, resulting in one value per subject representing frontal theta power modulation during the delay period, and one value representing parieto-occipital alpha power modulation, for both encoding and delay periods, although no significant inter-subject correlations were detected for the encoding period (see results). These values were then

submitted to the voxel-wise computation of Spearman's Rho, resulting in a whole-brain statistical map of areas in which individual differences in EEG reactivity predicted fMRI reactivity for increased levels of working memory load.

## LORETA Source estimation

In order to estimate the intracranial sources of the observed changes in EEG theta and alpha power, we used LORETA (Low Resolution Electromagnetic Brain Tomography, Pascual-Marqui et al., 1994), implemented in the freely available LORETA-KEY software (http://www.unizh.ch/keyinst/NewLORETA/LORETA01.htm). This technique produces a distributed linear inverse solution, in the form of a current density map, by minimizing the L2-norm of the difference between the predicted forward solution and the observed data, weighted by a Laplacian operator, which has the effect of producing as smooth an estimate as possible. While numerous strategies for 3D localization of EEG activity are available (Michel et al., 2004, Pascual-Marqui, 1999), the use of a smoothly distributed inverse solution facilitates combining results across subjects, similar to the smoothing of fMRI data in multi-subject studies. The algorithm for frequency-domain LORETA for localization of oscillatory activity differs slightly from its better-known time-domain equivalent, requiring a cross-spectral matrix as input, as described in Frei et al., (2001).

For each subject, a LORETA inverse transformation was computed from the locations of the electrodes retained in that individual's analyses (ranging from 112 to 125), using a standardized three-shell spherical head model registered to reference space (the MNI brain). EEG epochs from the encoding and delay periods were selected for frequency domain source localization. These were the same epochs used for spectral analysis of the individual channel EEG data (2.9 seconds for encoding, one epoch per trial, and 1.8 seconds for delay, five epochs per trial). The cross-spectral matrix was computed for each epoch and averaged within subject and condition, and then submitted to the inverse solution algorithm, resulting in a LORETA map for each frequency. LORETA maps were then exported to Analyze format using a freely available program (www.ihb.spb.ru/~pet_lab/L2S/L2SMain.htm), and imported into AFNI for further analysis and comparison with fMRI data. LORETA maps were averaged across frequencies into theta (4–7 Hz) and alpha (8–12 Hz) bands, and then a difference image for each subject and frequency band was computed by subtracting the 2-digit condition from the 6-digit condition, for both the encoding and delay periods. As with the fMRI data, the best single estimate of a linear load effect in each subject is simply the difference between the 6-digit and 2-digit conditions, which is exactly proportional to the magnitude of a linear regression coefficient estimated from all 3 conditions. The resulting difference maps were then averaged across subjects and superimposed on a common reference anatomical brain image for visualization, subject to statistical thresholding with a paired t-test. Multi-subject LORETA statistical maps were thresholded at the same voxel-wise threshold as fMRI maps ($p<.01$), but without cluster filtering. These maps represent a reasonable estimate of the central location of maximal power differences, but their precise spatial extent is not inherently meaningful, given the smoothness constraints of the LORETA algorithm. The goal of this analysis is not a definitive, high-precision definition of the generators of oscillatory activity, which is precluded by several factors: the spatial blurring of scalp EEG activity by the skull, the use of a standardized head model and electrode coordinates rather than models customized to individual subjects, and, importantly, the fact that oscillatory signals detectable in scalp recordings are likely to reflect activity coherent over a fairly large spatial scale (Nunez and Srinivasan, 2006). Nonetheless, the observed LORETA maxima provide a direct estimate of the spatial sources of oscillatory activity on the group level, suitable for comparison with fMRI maps obtained from the same cohort of subjects.

# RESULTS

## Behavioral

Repeated measures ANOVAs were conducted on the reaction time and accuracy of subjects' responses to probe digits in the Sternberg task, with session (MRI or EEG) and load (2,4, or 6 digits) as within-subject factors. As seen in figure 1B, there was a linear effect of increasing working memory load on reaction time [$F(34,2)=64.9$, $p < 1e\text{-}11$], with an average slope of 49 ms per additional digit. A modest effect of environment [$F(17,1)=6.15$, $p = .024$] and session X load interaction [$F(34,2)=4.15$, $p = .024$] are also seen, indicating that subjects were slightly faster to respond in the EEG session (32 ms on average), and that the slope with load was also slightly decreased. Average reaction time slopes were 57 ms per digit in the fMRI session alone, and 41 ms in the EEG session.

The faster reaction times in the EEG session are attributable to two factors, which cannot be separated. One factor is the physical environment, as most subjects find lying in the MRI scanner more tiring than the seated EEG environment. The other factor is a practice effect, as the MRI session was always conducted first. Practice effects could have been eliminated on the group level by counterbalancing the order of sessions across subjects, but as we were primarily interested in between-subject differences, we wanted to keep the session order the same in all subjects, so that individual differences in EEG and fMRI reactivity cannot trivially be attributed to that factor. Accuracy was at ceiling in all conditions (> 95%), and most subjects reported that their few errors were due to pressing the wrong button upon retrieval rather than forgetting the digits during the delay. Individual reaction time averages and reaction time slopes were calculated, but no significant correlations were observed between those factors and EEG or fMRI responses in the encoding and delay period. This is not surprising, given that behavioral data is obtained only from the retrieval phase of the Sternberg task, which was not the focus of this experiment. In verbal debriefing, all subjects were asked if they used any particular strategy to remember the digits. All subjects' reports were consistent with a strategy of rote rehearsal during the delay period; i.e. no exotic strategies such as mathematical manipulation of the digit strings were reported.

## FMRI group results, encoding period

The regression coefficients for a canonical hemodynamic response function timelocked to the onset of the digit array were submitted to a second-level multisubject analysis. The primary contrast of interest for this experiment is a linear effect of memory load, which, as described above, is optimally estimated as the difference between the 6-digit and 2-digit conditions. Therefore, this quantity was used both for construction of fMRI group activation maps and for computation of across-subjects correlations in EEG and fMRI load-dependent reactivity. A one-sample t-test of the load effect quantities for each subject (n=18) revealed load-dependent activation in a number of areas, including bilateral premotor cortex, dorsomedial prefrontal gyrus, inferior frontal gyri, superior temporal gyri, inferior parietal cortex, basal ganglia, and fusiform gyri (fig. 2A, Table 1A). As all significant clusters in this test are positive in sign, no encoding-related activity inversely correlated with memory load was detected.

## FMRI group results, delay period

Activation maps are based on models of overlapping hemodynamic responses to the encoding, delay, and probe phases of the task. The regression coefficients corresponding to delay period activity in the 6-digit and 2-digit conditions were subtracted and submitted to a one-sample t-test across subjects. Sustained load-dependent activation was detected in many of the same regions as in the encoding contrast (fig. 2B, Table 1B). To confirm the accuracy of the activation maps based on hemodynamic models, we also examined the empirically estimated BOLD timecourses derived from the deconvolution analysis. Timecourses were averaged across all

voxels in certain activation clusters, circled in fig. 2B. In the timecourse plots of figure 2C–D, vertical lines indicate the time period in which the majority of the modeled signal was attributable to delay activity. Examination of activation timecourses in two positively activated regions (fig. 2C–D) shows that the BOLD signal increases following the onset of the stimuli, and remains elevated in the high-load conditions while the subject is rehearsing the digits, until the presentation of the probe digit, when the signal increases again. Additionally, this test identified areas in which BOLD signal during the delay period is negatively correlated with memory load, including the right inferior parietal lobe and the left superior temporal gyrus (fig. 2B). Timecourse plots demonstrate that these areas undergo a sustained load-dependent suppression of the BOLD signal during the delay period, in the absence of a discernible phasic activation peak corresponding to the encoding phase (fig. 2E–F).

### Test of Linearity of load modulated responses

As explained in the methods section, the linear effect of memory load in each individual subject is optimally estimated as the difference between the two extreme levels (6 and 2 digits), given three equally spaced levels in the experiment. Nonetheless, using only this quantity for further analyses can be considered adequate only if the effect of memory load is approximately linear, i.e. the 4-digit condition falls approximately half-way between the other two conditions. To exclude the possibility of a “U-shaped” relationship to memory load, we also examined the results of a 3-level repeated measures ANOVA on BOLD signal related to the encoding and delay epochs. The resulting activation maps (not shown) were almost identical to the results obtained from the simple 6-minus-2 subtraction. We did not detect any areas exhibiting significant effects of memory load, in which the 4-digit condition was significantly higher or lower than the other two conditions. Therefore, the use of a single representative value for memory load effects appears to be well justified.

### EEG theta power reactivity

Given previous reports of Fm theta activity in memory tasks, we hypothesized that some subjects would show an increase in theta power during the delay period at greater levels of memory load. The most probable location for such an increase would be at electrodes located in the anterior midline region, corresponding to location Fz in the international 10–20 system. Given that Jensen et al. (2002) observed such an effect in only one out of ten subjects, we expected that only a minority of our 18 subjects would exhibit the effect strongly, but that a quantification of the effect size in each subject might correlate with fMRI reactivity. In Figure 3A–C, we show an independent component from one subject that clearly expresses a frontal midline theta rhythm that is strongly modulated by memory load. Figure 3A shows the scalp projection of this component, indicating that it captures variance in the EEG signal shared by electrodes in the frontal midline region. Figure 3B displays the average timecourse of theta power (4–7 Hz) for this component in each condition, demonstrating that there is a load-dependent power increase specific to the delay period. Figure 3C displays the average power spectra for this component during the delay period, showing that peak power, as well as the load-dependent increase, is concentrated in the theta band specifically (in this case approximately 4–8 Hz, peaking at 5.5 Hz), with relatively little contribution from the alpha band that typically dominates the scalp EEG.

Although the EEG activity shown in Figure 3A–C conforms closely to our pre-existing notion of memory load-modulated Fm theta, it is not a robust pattern across the cohort of subjects. While some other subjects do exhibit increased Fm theta power with greater memory load, only one subject exhibited a single IC with all of the characteristics of the hypothesized load-modulated Fm theta generator: peak power in the theta band with no accompanying alpha peak, modulated by memory load in the delay period, and a scalp distribution confined to the frontal midline region. Figure 3D displays a topographic map of the group average regression

coefficient for memory load on delay period power in the theta band. A single cluster of positive coefficients appears in the predicted frontal midline location. However, the positive values for electrodes in this region are driven by strong effects in a minority of subjects and do not reach statistical significance in random effects analysis across the cohort ($p > .3$). Nonetheless, the inter-subject variability of theta power reactivity in this region is of key interest to the question of whether load-dependent theta increases relate to fMRI responses. Therefore, we defined a frontal midline ROI including eight electrodes centered on the Fz location (indicated by the black ellipse in Figure 3D, for examination of EEG-fMRI correlations. These eight electrodes were chosen to encompass the region of maximal theta power increase in the group. For each subject, we computed a single theta power regression score by averaging together the regression coefficients for memory load on delay-period theta power across the channels comprising the ROI. Next, for each voxel in the brain, we computed Spearman's rank-order correlation coefficient ("Rho") between the EEG delay-period theta power load effect and the fMRI delay period load effect across the 18 subjects, and thresholded the resulting statistical map in the usual manner.

This test revealed four significant clusters of correlation between load effects in theta power and BOLD (Table 1C), all of which were negative, suggesting that an increase in theta power may reflect a decrease in the BOLD signal within certain regions. The largest cluster of correlation was located within anterior medial prefrontal cortex (Figure 3H), consistent with the hypothesized sources of theta rhythm (see discussion). Additional areas of correlation were located in left and right lateral parietal cortex, approximately corresponding to the angular gyri (Figure 3E), while a fourth cluster was located in the left middle prefrontal gyrus, close to the larger medial prefrontal cluster. Scatter plots of average EEG and fMRI load scores for the right angular gyrus and medial prefrontal clusters are shown in Figure 3F and 3I, illustrating the pattern of across-subjects correlations. The single subject with the largest Fm theta modulation effect (whose IC is shown in fig. 3A–C) is the outlier on the right of the scatterplots, and does not drive the correlation, but rather reduces it.

In order to evaluate the observed pattern of EEG-fMRI correlation, we compared it with a source estimate of EEG power modulation computed directly from the EEG data, irrespective of the fMRI results. We performed source estimates of theta and alpha power during the 6-digit and 2-digit conditions in each subject during the delay period, using the LORETA algorithm, and submitted the resulting maps to a paired t-test across subjects. Thus, a whole-brain statistical map was produced of the average load effect across subjects. As the load effect was not statistically significant in the electrode spectra across subjects, we did not expect this procedure to yield any significant clusters; the intent was to use the unthresholded map to locate the maxima of theta increases. In fact, however, one significant cluster was detected, located in anterior medial prefrontal cortex (Figure 3G). This region overlaps the cluster of significant theta-BOLD correlation, but does not overlap any region of positive BOLD increments with memory load. There was no indication of any theta power increase in lateral frontal or parietal regions, even at very liberal thresholds. Thus, the source estimation results are consistent with existing findings that load-modulated theta power is generated in the vicinity of the medial prefrontal cortex and ventral anterior cingulate (Asada et al., 1999, Ishii et al., 1999). The fact that the LORETA algorithm detected significant increases in theta that were not significant on the electrode level may be because the power values for scalp electrodes are affected by multiple intracranial generators that can cancel each other out when power spectra are computed, but are dissociable in source-space analysis, as the LORETA algorithm takes into account information about the phase relationships between electrodes, rather than basing estimates on the power spectra at each electrode individually.

### EEG alpha power reactivity

Although elucidation of the relationship between theta-band activity and BOLD was the initial goal of this study, we also observed striking EEG dynamics related to memory load in the alpha band (8–12 Hz), which warranted further analysis. Upon presentation of the digit array, there was a very consistent drop in posterior alpha power. Furthermore, the degree to which alpha power decreased was monotonically related to the number of digits in the array. During the delay period, however, there was no consistent relationship between memory load and alpha power, but there were striking effects within individual subjects. As an illustration of these effects, we present data characterizing the behavior of a particular IC in two example subjects. Figures 4A and 4D display the scalp maps of a component in two subjects, both of which display a topography typical of a right-lateralized posterior alpha rhythm generator. Figures 4Band 4E display the averaged timecourses of alpha power (8–12 Hz) for these two components in each condition. As seen in most subjects, both components exhibit a strong decrease in alpha power upon presentation of the digit array, and this decrease is larger with more digits. During the delay period, however, the behavior of the two components differs. In the first subject (figure 4B–C), alpha power returns almost to baseline levels during the delay period, but remains somewhat depressed in the conditions with greater memory load. In the second subject (figure 4E–F), alpha power also returns approximately to baseline levels, but is actually higher during trials with greater memory load, the reverse of the pattern seen during the encoding period. Figures 4C and 4F display the average power spectra for these two components in the delay period. The within-subject statistical significance of these differences was confirmed by inspecting the jackknifed 95% confidence intervals (Thomson and Chave, 1990) for each spectrum (not shown), confirming that they are not simply attributable to random fluctuations between trials.

Given that different patterns of posterior alpha power reactivity are observed across subjects, we hypothesized that these differences might correlate with fMRI reactivity as well, as seen for frontal theta power. In order to choose the scalp electrodes to use in the EEG-fMRI correlation analysis, we examined the topographical maps of the group average regression coefficient for memory load on alpha power in the encoding and delay periods. These are displayed in Figure 4G–H. These maps indicated that load-dependent alpha power modulation occurred primarily over parietal-occipital electrodes in both time periods. For EEG-fMRI correlation analysis, we selected a broad region covering 24 electrodes that exhibited maximal load modulation, indicated by the red ellipse in Figure 4G and 4H. The regression coefficients for memory load on alpha power were averaged across the electrodes in this region and submitted to multisubject statistical analysis. Load modulation was highly significant for the encoding period [$t(17) = -3.91$, $p < .002$], but not for the delay period [$t(17) = -0.86$, $p > .4$]. While load effects were consistently negative during encoding, the delay period scores were positive in half of the subjects and negative in half. Regression scores for EEG posterior alpha power were submitted, along with voxel-wise fMRI regression coefficients, to calculation of Spearman's Rho for the encoding and delay periods. No significant correlations were detected for the encoding period, which is not surprising given the relative lack of intersubject variability. In the delay period, however, one significant correlation cluster of was detected, which was negative in sign and located within the precuneus/parietal-occipital junction (Figure 4I–J). In fMRI considered alone, this region was not significantly activated or deactivated on the group level by differing levels of memory load. Examination of the scatter plot in Figure 4J suggests that this region can be either positively or negatively activated by increased levels of memory load in different subjects, and that positive activation of this region is associated with decreases in alpha power (and vice-versa).

We also sought to confirm the localization of EEG-fMRI correlation in the alpha band with direct source localization of alpha activity with the LORETA algorithm. Therefore, load effect

subtraction maps (6-digit minus 2-digit) averaged in the alpha band were submitted to a voxel-wise 1-sample t-test, as done for the theta band. In the delay period, no significant clusters were detected, which is not surprising, given the high inter-subject variance. As subjects exhibit strong decreases in alpha power while others exhibit increases, these would cancel each other out on the group level, making it impossible to use a group averaged difference map to localize the activity. In the encoding period, however, the load-modulated alpha power decrease was highly consistent across subjects, and was therefore easily localized with the LORETA procedure. Only one significant negative cluster emerged, located in the parietal-occipital region (Figure 4K), and overlapping with the cluster of EEG-fMRI correlation. Thus, to the extent that we are able to estimate the source of load-modulated alpha activity from these data, the direct source localization seems to correspond closely to the observed site of EEG-fMRI correlation. Of course, we cannot be certain that the sources of alpha power modulation during the encoding and delay periods are the same. However, the available evidence suggests that they are, given that the average scalp topographies of load modulation in the encoding and delay periods appear quite similar, albeit very different in magnitude (Figure 4G–H), and that the same independent components tend to reflect load modulation during both periods (Figure 4A–F). We note that strong lateral parietal-occipital sources of alpha power were also identified in the LORETA solutions, but that activity in those regions was not modulated significantly by memory load. Therefore, the localization of load-modulated alpha power to a posterior midline region does not simply reflect a failure of the inverse solution to reveal bilaterally symmetric lateral sources. Rather, it appears that load modulation of alpha power is primarily a property of the midline region, while lateralized alpha sources may reflect independent neural processes.

## DISCUSSION

The present study used a well known working memory task to investigate the relationship between EEG oscillations and BOLD signal changes, through the examination of between-subjects correlations. While inter-individual variability in EEG spectral properties has often been reported (e.g. Inanaga, 1990, Fingelkurts, 2005), this study is, to our knowledge, the first to investigate quantitative relationships between EEG and a second neuroimaging modality on the group level. We found that memory load-dependent power increases in the theta and alpha ranges were both correlated negatively with BOLD activations, which is to say that a load-induced increase in power corresponds to a decrease in BOLD. The presence of a negative correlation in these frequency ranges is largely consistent with a growing body of data on frequency dependent correlations between oscillatory field potentials and hemodynamic signals. Mukamel et al. (2005), examining fMRI and intracranial EEG signals in the human auditory cortex induced by viewing a movie, reported negative correlations at frequencies below 20 Hz, and positive correlations at higher frequencies. Consistent with that dissociation, other studies (Niessing et al., 2005, Lachaux et al., 2007) have reported positive relationships between the gamma band and BOLD, while numerous studies have detected negative correlations between alpha band activity and cortical BOLD in simultaneous EEG-fMRI ((Goldman et al., 2002, Moosmann et al., 2003, Laufs et al., 2003, 2006, de Munck et al., 2007). Using MEG and fMRI in separate sessions, Brookes et al. (2005) demonstrated that positive BOLD responses induced by visual stimulation in occipital cortex colocalized with alpha decreases and gamma increases, providing further support for a general frequency dependence in the relationship between oscillatory neuronal amplitude and the BOLD signal, as predicted by a recent modeling study (Kilner et al., 2005). Nonetheless, empirical evidence for a strict frequency dependence is equivocal, as some instances of positive correlation between alpha oscillations and BOLD within individual subjects have been reported (Goncalves et al., 2006, de Munck et al., 2007), and both positive and negative relationships with theta rhythm have been reported at the group level (Sammer et al., 2006, Mizuhara et al., 2004, Winterer et al., 2007).

Unlike some previous studies that have employed simultaneous EEG-fMRI during states of unconstrained rest or continuous mental arithmetic, we recorded EEG and fMRI in separate sessions, using an event-related paradigm with strictly defined temporal epochs. Therefore, several concerns must be addressed in order to interpret across-subject correlations derived from EEG and fMRI measured in separate sessions. One potential problem is the presence of a practice effect. Subjects may perform a task differently the second time compared with the first time – as reflected by the slightly faster reaction times observed in the second session in this study. For that reason, we elected not to counterbalance the order of the fMRI and EEG sessions across subjects, but rather to consistently conduct the fMRI first. The presence of a consistent practice effect is independent of inter-subject variability, and therefore does not confound the finding of across-subject correlations. Variability in the extent of the practice effect may exist across subjects, but this would simply add to other sources of variance in decreasing the power of the study to find a significant effect, rather than invalidating effects that are found.

A second concern is the reproducibility of fMRI and EEG measurements. Here again, the effect of intra-subject variability between sessions does not confound the findings of this study, but simply reduces its power to reveal stable inter-subject differences. The presence of significant between-subjects correlations suggests that individual subjects do exhibit specific physiological patterns that are robust enough to be detectable in multiple modalities measured in separate sessions. Additionally, previous studies suggest that the reproducibility of individual patterns of EEG spectral modulation is relatively high compared to inter-subject variance (McKevoy et al., 2000, Fingelkurts, 2005), while test-retest fMRI studies have reached shown reasonable repeatability in working-memory related activity (Manoach et al., 2001, Wei et al., 2004, c.f. Marshall et al., 2004). In a pilot study using a slightly different version of the Sternberg task, we observed consistent individualized patterns of alpha and theta modulation in three subjects across two sessions (Meltzer et al., 2004), thus prompting us to explore this variability further with the full-scale multimodal study that is reported here.

A third concern is that the individual differences approach can only reveal relationships between effects that have a relatively high intersubject variance. In this study, for example, only a minority of subjects exhibited load-dependent fMRI deactivation of medial prefrontal cortex, and these same subjects tended to exhibit frontal theta power increases as well. Other effects were much more consistent across the cohort, such as load-modulated positive BOLD responses in premotor and parietal areas, and alpha desynchronization during the encoding period. It is likely that inter-subject variation in these measures is not high enough to reveal correlations, even if, in fact, physiological relationships do exist. Once again, this limitation reflects a lack of power in this study to reveal certain relationships, not an invalidation of its actual findings. An examination of between-subjects correlations such as this provides complementary information to studies of effects that are more consistent across subjects. An effect that is highly consistent across subjects may achieve statistical significance in both EEG and fMRI modalities, but may not provide any information on the relationship between the two forms of signal. A highly variable effect, on the other hand, may fail to reach statistical significance on the cohort level, as is the case for the theta and alpha effects during the delay period in this study, but may in fact yield a significant correlation between the two modalities, providing insight into how they are related, as we have shown here. Therefore, it is our hope that this finding may spur more interest in between-subject variability that is commonly dismissed as “noise.”

As discussed in the introduction, theta oscillations have traditionally been viewed as indexing an active state of cognitive demand, and thus it is somewhat surprising that they should be anticorrelated with BOLD, which is also well established as an indicator of neuronal activity of cognitive relevance. Our source localization estimates placed the generators of load-

modulated Fm theta in the vicinity of the medial prefrontal cortex and anterior cingulate, in agreement with many other studies of theta oscillations (Ishii et al., 1999, Tsujimoto et al., 2006, Luu et al., 2004, Onton et al., 2005, Asada et al., 1999). This region forms part of the default mode network, which is commonly deactivated in cognitive tasks. Notably, other regions that were negatively correlated with theta modulation in this study included the bilateral angular gyri, which are also components of the default mode network. These results suggest that the Fm theta increases commonly observed in cognitive tasks may actually relate to the "task-induced deactivation" of these regions, rather than to the "task-positive" regions that are located more laterally.

Given that increased theta oscillation is associated with cognitive information processing, the observed association with negative BOLD responses raises the possibility that negative BOLD signals in default mode regions may reflect neuronal activity of cognitive relevance, rather than a suppression of ongoing unrelated activity as is commonly thought. While evidence suggests that some cases of negative BOLD may reflect non-neuronal processes such as "vascular steal" (Harel et al., 2002), multimodal studies have indicated that, in many cases, negative BOLD signals reflect genuine decreases in quantities associated with neuronal energy use, including cerebral blood flow and oxygen metabolism (Stefanovic et al., 2004, Shmuel et al., 2002). Furthermore, negative BOLD responses in visual cortex have been shown to correspond directly to decreases in neuronal spike rates arising from lateral inhibition (Shmuel et al., 2006) and to reflect specific stimulus-related properties (Bressler et al., 2007). In view of these results, it is likely that the particular form of neuronal information processing that is characterized by increased generation of theta oscillations is largely inhibitory in character, resulting in a decrease in metabolic indices such as BOLD.

Numerous findings in the animal literature support such a negative link between theta and metabolism. Two studies have demonstrated a negative correlation between theta power and glucose metabolism as measured by autoradiographic techniques in rodents (Uecker et al., 1997, Sanchez-Arroyos et al., 1993). Furthermore, several recent studies have examined the relationship between spike timing and theta rhythm, showing that *spike timing*, but not necessarily *spike rate*, in rodent medial prefrontal cortex is closely linked to hippocampal theta rhythm, (Jones and Wilson, 2006, Siapas et al., 2005, Hyman et al., 2005). In the primate, Lee et al. (2005) demonstrated that theta-locked spike timing occurs in the delay period of a working memory task in the absence of increased firing rates, which occur rather during the encoding and recall phases of the task. Finally, Wang et al. (2005), recording from the cortex of human surgery patients, demonstrated theta increases in the anterior cingulate during a variety of cognitive tasks, accompanied by decreased multi-unit spiking.

Reports of negative correlations between local field power and BOLD in low frequency ranges may seem somewhat surprising, given the well-known finding of Logothetis et al. (2001), that stimulus-induced increases in local field power match BOLD increases more closely than do increases in multi-unit spiking. However, Logothetis et al. (2001) did not distinguish between oscillatory power in the different frequency bands that comprise EEG. The multitude of frequency-specific responses observed in scalp and invasive EEG experiments have established that local field power is not a unitary phenomenon, and that the relationship between power and metabolism is likely to be markedly frequency dependent. Findings of negative correlations between theta power and metabolic indices suggest that theta oscillations may be an electrophysiological index of inhibitory activity that plays a key role in cognition. Given the wide array of cognitive tasks that have been shown to elicit theta oscillations (as well as negative BOLD responses), the exact nature of the information processing role played by theta remains to be elucidated, although numerous theoretical models have been proposed (e.g. Lengyel et al., 2005, Hasselmo, 2005, Bland and Oddie, 2001).

The high inter-subject variance of load-dependent deactivation in default mode regions, and of the associated theta power increase, suggest that the two effects reflect the recruitment of a neurocognitive system that is not essential for task performance in all subjects. This is consistent with a recent report (Greicius and Menon, 2004) demonstrating that coordinated default mode activity is often detectable through independent component analysis of fMRI data, but is only anticorrelated with task-induced lateral activations some of the time. Presently, it is not known whether this variability is correlated with other subject-specific characteristics, which may reflect differences in cognitive strategy or even personality. Personality characteristics such as extroversion/introversion and IQ have been observed to correlate with activation in working memory tasks (Gray and Braver, 2002, Kumari et al., 2004, Habeck et al., 2005), while associations between theta power and personality have also been reported (Inanaga, 1998). In the current study, we did not observe any correlations between the physiological measurements and behavioral variability between subjects. In informal debriefing, all subjects reported using similar strategies of subvocal rehearsal to remember the digits. However, it is important to note that the only observable behavior in this task is the button-press response to the probe digit, and that the subjects did not perform any overt responses during the encoding and delay phases that are the focus of this study. Consequently, other tasks may be better suited to revealing a relationship between individual variability of EEG dynamics and behavioral consequences.

The effects in the alpha band observed in this study are generally consistent with the prevailing view of alpha oscillations as an indicator of cortical “idling.” As discussed above, alpha amplitude typically decreases under conditions of greater stimulation and cognitive demand. In this study, we observed a highly consistent pattern of load-dependent alpha suppression during the encoding period, in that digit arrays with more digits in them suppressed alpha power to a greater extent. Source localization estimates placed the locus of this effect in the vicinity of the posterior cingulate and parieto-occipital junction. This localization agrees well with other studies that have attempted to localize task-modulated alpha oscillations. While alpha is thought to be generated in numerous regions of the cortex, this region is consistently identified as one of its strongest generators (Ciulla et al., 1999, Yamagishi et al., 2003), and Vanni et al. (1997) reported that only alpha from this source was strongly modulated by cognitive task conditions. Similarly, Tuladhar et al. (2007), using beamforming analysis of MEG data, detected memory load-dependent increases in alpha power during a Sternberg task with face pictures as stimuli, and localized those increases to parietal-occipital midline cortex. This power increase was interpreted as inhibitory suppression of this region, rather than computational activity directly involved in memory retention. The present results support that interpretation, in that memory load-dependent increases in alpha power arising from parietal-occipital midline sources are seen to correlate negatively with the BOLD signal, which is usually thought of as a direct indicator of increased neuronal information processing.

While our results serve to further generalize the pattern of observed negative correlations between BOLD and alpha rhythm, we caution that they do not indicate any one-to-one correspondence between BOLD activation and alpha suppression in cognitive tasks. In fact, two salient dissociations between the two phenomena are observed in this study. First, we observed extensive positive BOLD activation in bilateral frontal and parietal regions related to increased working memory load, which is consistent with a large number of previous fMRI studies. However, there was no evidence of any alpha power suppression arising from these areas. It is possible that generation of task modulated alpha power is limited to a few areas of the cortex, such as the parieto-occipital midline regions, or that alpha oscillations in other regions are more subject to cancellation of extracranial electric fields due to the presence of counteroriented dipoles, making them relatively invisible to EEG. In any case, these findings suggest that the majority of positive BOLD activations may bear no relation to modulations of oscillatory power detectable in EEG/MEG recordings. Second, the only memory load related

effect in EEG that was consistent across the cohort of subjects was a suppression of alpha power at posterior midline electrodes during the encoding period, which was localized to a parieto-occipital midline source. While load-dependent BOLD modulation in this region was correlated negatively with alpha power during the delay period, we did not observe any consistent load modulation in that region's BOLD signal for the encoding period. Thus, the load-dependent alpha suppression during encoding appears to have no corresponding effect in fMRI. The two examples discussed here thus emphasize the independence and complementarity of EEG and fMRI measurements, with the first being an example of an fMRI effect with no corresponding EEG correlate, and the second an EEG effect with no fMRI correlate.

All together, the results of this study suggest that memory load induced increases in the theta and alpha frequency ranges may correspond to negative BOLD responses in certain cases, but that both EEG and fMRI effects may also occur independently of each other, such that the two modalities provide complementary information. Furthermore, the findings of across-subject correlations between the two modalities demonstrates the feasibility of using inter-subject variability as a tool for probing the relationship between different kinds of signals in multimodal brain imaging. This is particularly true for cases in which striking effects are seen in some individual subjects but do not generalize to the population at large. In such cases, examination of correlations with an independent variable can help to reveal information relevant to understanding the nature of the effect. In this study, we have seen that Fm theta increases induced by greater levels of memory load relate to deactivation in "default mode" structures of the brain. While numerous studies have demonstrated increases in Fm theta that are consistent across subjects, data on the relationship of such effects to the BOLD signal has been difficult to obtain. In choosing a task with a high level of inter-subject variance for multimodal exploration, quantitative relationships across modalities can be detected that would not otherwise be apparent. Therefore, we hope that this study may spur greater interest in inter-individual variations that are commonly observed, but seldom studied systematically.

**Acknowledgements**

This research was supported by NIH R01-NS051622 (RTC), by training fellowships from the American Epilepsy Society (JAM, MN), NIDA grants RO1-DA-06025 (LCM), DA-017863 (LCM) and KO5 (LCM) and grants from NICHD P01-HD03008 and an unrestricted educational grant from Pfizer Inc. Additionally, the work was supported in part by the Yale Children's Clinical Research Center grant MO1-RR06022, General Clinical Research Centers Program, National Center for Research Resources, NIH. We thank Michael Crowley and Eric Langlois for assistance in EEG data acquisition.

## References

Asada H, Fukuda Y, Tsunoda S, Yamaguchi M, Tonoike M. Frontal midline theta rhythms reflect alternative activation of prefrontal cortex and anterior cingulate cortex in humans. Neurosci Lett 1999;274:29–32. [PubMed: 10530512]

Bastiaansen M, Hagoort P. Event-induced theta responses as a window on the dynamics of memory. Cortex 2003;39:967–992. [PubMed: 14584562]

Bastiaansen MC, Posthuma D, Groot PF, de Geus EJ. Event-related alpha and theta responses in a visuo-spatial working memory task. Clin Neurophysiol 2002;113:1882–1893. [PubMed: 12464325]

Bastiaansen MC, van Berkum JJ, Hagoort P. Event-related theta power increases in the human EEG during online sentence processing. Neurosci Lett 2002;323:13–16. [PubMed: 11911979]

Bland BH, Oddie SD. Theta band oscillation and synchrony in the hippocampal formation and associated structures: the case for its role in sensorimotor integration. Behav Brain Res 2001;127:119–136. [PubMed: 11718888]

Bressler D, Spotswood N, Whitney D. Negative BOLD fMRI Response in the Visual Cortex Carries Precise Stimulus-Specific Information. PLoS ONE 2007;2:e410. [PubMed: 17476332]

Brookes MJ, Gibson AM, Hall SD, Furlong PL, Barnes GR, Hillebrand A, Singh KD, Holliday IE, Francis ST, Morris PG. GLM-beamformer method demonstrates stationary field, alpha ERD and gamma ERS co-localisation with fMRI BOLD response in visual cortex. Neuroimage 2005;26:302–308. [PubMed: 15862231]

Burgess AP, Gruzelier JH. Short duration power changes in the EEG during recognition memory for words and faces. Psychophysiology 2000;37:596–606. [PubMed: 11037036]

Ciulla C, Takeda T, Endo H. MEG characterization of spontaneous alpha rhythm in the human brain. Brain Topogr 1999;11:211–222. [PubMed: 10217445]

Cohen MS. Parametric analysis of fMRI data using linear systems methods. Neuroimage 1997;6:93–103. [PubMed: 9299383]

de Munck JC, Goncalves SI, Huijboom L, Kuijer JP, Pouwels PJ, Heethaar RM, Lopes da Silva FH. The hemodynamic response of the alpha rhythm: An EEG/fMRI study. Neuroimage 2007;35:1142–1151. [PubMed: 17336548]

Delorme A, Makeig S. EEGLAB: an open source toolbox for analysis of single-trial EEG dynamics including independent component analysis. J Neurosci Methods 2004;134:9–21. [PubMed: 15102499]

Fingelkurts AA. Stability, reliability and consistency of the compositions of brain oscillations. Int J Psychophysiol. 2005

Forman SD, Cohen JD, Fitzgerald M, Eddy WF, Mintun MA, Noll DC. Improved assessment of significant activation in functional magnetic resonance imaging (fMRI): use of a cluster-size threshold. Magn Reson Med 1995;33:636–647. [PubMed: 7596267]

Fox MD, Snyder AZ, Vincent JL, Corbetta M, Van Essen DC, Raichle ME. The human brain is intrinsically organized into dynamic, anticorrelated functional networks. Proc Natl Acad Sci U S A 2005;102:9673–9678. [PubMed: 15976020]

Fransson P. How default is the default mode of brain function? Further evidence from intrinsic BOLD signal fluctuations. Neuropsychologia 2006;44:2836–2845. [PubMed: 16879844]

Frei E, Gamma A, Pascual-Marqui R, Lehmann D, Hell D, Vollenweider FX. Localization of MDMA-induced brain activity in healthy volunteers using low resolution brain electromagnetic tomography (LORETA). Hum Brain Mapp 2001;14:152–165. [PubMed: 11559960]

Friston KJ, Holmes AP, Worsley KJ. How many subjects constitute a study? Neuroimage 1999;10:1–5. [PubMed: 10385576]

Gevins A, Smith ME, McEvoy L, Yu D. High-resolution EEG mapping of cortical activation related to working memory: effects of task difficulty, type of processing, and practice. Cereb Cortex 1997;7:374–385. [PubMed: 9177767]

Gevins AS, Zeitlin GM, Doyle JC, Yingling CD, Schaffer RE, Callaway E, Yeager CL. Electroencephalogram correlates of higher cortical functions. Science 1979;203:665–668. [PubMed: 760212]

Goldman RI, Stern JM, Engel J Jr, Cohen MS. Simultaneous EEG and fMRI of the alpha rhythm. Neuroreport 2002;13:2487–2492. [PubMed: 12499854]

Goncalves SI, de Munck JC, Pouwels PJ, Schoonhoven R, Kuijer JP, Maurits NM, Hoogduin JM, Van Someren EJ, Heethaar RM, Lopes da Silva FH. Correlating the alpha rhythm to BOLD using simultaneous EEG/fMRI: inter-subject variability. Neuroimage 2006;30:203–213. [PubMed: 16290018]

Gray JR, Braver TS. Personality predicts working-memory-related activation in the caudal anterior cingulate cortex. Cogn Affect Behav Neurosci 2002;2:64–75. [PubMed: 12452585]

Greicius MD, Menon V. Default-mode activity during a passive sensory task: uncoupled from deactivation but impacting activation. J Cogn Neurosci 2004;16:1484–1492. [PubMed: 15601513]

Guderian S, Duzel E. Induced theta oscillations mediate large-scale synchrony with mediotemporal areas during recollection in humans. Hippocampus 2005;15:901–912. [PubMed: 16161060]

Gundel A, Wilson GF. Topographical changes in the ongoing EEG related to the difficulty of mental tasks. Brain Topogr 1992;5:17–25. [PubMed: 1463655]

Habeck C, Rakitin BC, Moeller J, Scarmeas N, Zarahn E, Brown T, Stern Y. An event-related fMRI study of the neural networks underlying the encoding, maintenance, and retrieval phase in a delayed-match-to-sample task. Brain Res Cogn Brain Res 2005;23:207–220. [PubMed: 15820629]

Harel N, Lee SP, Nagaoka T, Kim DS, Kim SG. Origin of negative blood oxygenation level-dependent fMRI signals. J Cereb Blood Flow Metab 2002;22:908–917. [PubMed: 12172376]

Hasselmo ME. What is the function of hippocampal theta rhythm?--Linking behavioral data to phasic properties of field potential and unit recording data. Hippocampus 2005;15:936–949. [PubMed: 16158423]

Hyman JM, Zilli EA, Paley AM, Hasselmo ME. Medial prefrontal cortex cells show dynamic modulation with the hippocampal theta rhythm dependent on behavior. Hippocampus 2005;15:739–749. [PubMed: 16015622]

Inanaga K. Frontal midline theta rhythm and mental activity. Psychiatry Clin Neurosci 1998;52:555–566. [PubMed: 9895201]

Ishii R, Shinosaki K, Ukai S, Inouye T, Ishihara T, Yoshimine T, Hirabuki N, Asada H, Kihara T, Robinson SE, Takeda M. Medial prefrontal cortex generates frontal midline theta rhythm. Neuroreport 1999;10:675–679. [PubMed: 10208529]

Jensen O, Gelfand J, Kounios J, Lisman JE. Oscillations in the alpha band (9–12 Hz) increase with memory load during retention in a short-term memory task. Cereb Cortex 2002;12:877–882. [PubMed: 12122036]

Jensen O, Tesche CD. Frontal theta activity in humans increases with memory load in a working memory task. Eur J Neurosci 2002;15:1395–1399. [PubMed: 11994134]

Jha AP, McCarthy G. The influence of memory load upon delay-interval activity in a working-memory task: an event-related functional MRI study. J Cogn Neurosci 2000;12(Suppl 2):90–105. [PubMed: 11506650]

Jones MW, Wilson MA. Theta rhythms coordinate hippocampal-prefrontal interactions in a spatial memory task. PLoS Biol 2005;3:e402. [PubMed: 16279838]

Kilner JM, Mattout J, Henson R, Friston KJ. Hemodynamic correlates of EEG: a heuristic. Neuroimage 2005;28:280–286. [PubMed: 16023377]

Kirschen MP, Chen SH, Schraedley-Desmond P, Desmond JE. Load- and practice-dependent increases in cerebro-cerebellar activation in verbal working memory: an fMRI study. Neuroimage 2005;24:462–472. [PubMed: 15627588]

Klimesch W, Doppelmayr M, Russegger H, Pachinger T. Theta band power in the human scalp EEG and the encoding of new information. Neuroreport 1996;7:1235–1240. [PubMed: 8817539]

Klimesch W, Doppelmayr M, Schwaiger J, Auinger P, Winkler T. 'Paradoxical' alpha synchronization in a memory task. Brain Res Cogn Brain Res 1999;7:493–501. [PubMed: 10076094]

Kumari V, ffytche DH, Williams SC, Gray JA. Personality predicts brain responses to cognitive demands. J Neurosci 2004;24:10636–10641. [PubMed: 15564579]

Lachaux JP, Fonlupt P, Kahane P, Minotti L, Hoffmann D, Bertrand O, Baciu M. Relationship between task-related gamma oscillations and BOLD signal: New insights from combined fMRI and intracranial EEG. Hum Brain Mapp 2007;1:1.

Laufs H, Holt JL, Elfont R, Krams M, Paul JS, Krakow K, Kleinschmidt A. Where the BOLD signal goes when alpha EEG leaves. Neuroimage. 2006

Laufs H, Kleinschmidt A, Beyerle A, Eger E, Salek-Haddadi A, Preibisch C, Krakow K. EEG-correlated fMRI of human alpha activity. Neuroimage 2003;19:1463–1476. [PubMed: 12948703]

Lee H, Simpson GV, Logothetis NK, Rainer G. Phase locking of single neuron activity to theta oscillations during working memory in monkey extrastriate visual cortex. Neuron 2005;45:147–156. [PubMed: 15629709]

Lengyel M, Huhn Z, Erdi P. Computational theories on the function of theta oscillations. Biol Cybern 2005;92:393–408. [PubMed: 15900483]

Logothetis NK, Pauls J, Augath M, Trinath T, Oeltermann A. Neurophysiological investigation of the basis of the fMRI signal. Nature 2001;412:150–157. [PubMed: 11449264]

Luu P, Tucker DM, Makeig S. Frontal midline theta and the error-related negativity: neurophysiological mechanisms of action regulation. Clin Neurophysiol 2004;115:1821–1835. [PubMed: 15261861]

Makeig S. Auditory event-related dynamics of the EEG spectrum and effects of exposure to tones. Electroencephalogr Clin Neurophysiol 1993;86:283–293. [PubMed: 7682932]

Manoach DS, Halpern EF, Kramer TS, Chang Y, Goff DC, Rauch SL, Kennedy DN, Gollub RL. Test-retest reliability of a functional MRI working memory paradigm in normal and schizophrenic subjects. Am J Psychiatry 2001;158:955–958. [PubMed: 11384907]

Marshall I, Simonotto E, Deary IJ, Maclullich A, Ebmeier KP, Rose EJ, Wardlaw JM, Goddard N, Chappell FM. Repeatability of motor and working-memory tasks in healthy older volunteers: assessment at functional MR imaging. Radiology 2004;233:868–877. [PubMed: 15498902]

McEvoy LK, Smith ME, Gevins A. Test-retest reliability of cognitive EEG. Clin Neurophysiol 2000;111:457–463. [PubMed: 10699407]

Meltzer, JA.; Zaveri, HP.; Spencer, SS.; Spencer, DD.; Constable, RT. Human Brain Mapping. Budapest; Hungary: 2004. Individual variability in spectral correlates of working memory load in scalp and intracranial recordings.

Michel CM, Murray MM, Lantz G, Gonzalez S, Spinelli L, Grave de Peralta R. EEG source imaging. Clin Neurophysiol 2004;115:2195–2222. [PubMed: 15351361]

Miezin FM, Maccotta L, Ollinger JM, Petersen SE, Buckner RL. Characterizing the hemodynamic response: effects of presentation rate, sampling procedure, and the possibility of ordering brain activity based on relative timing. Neuroimage 2000;11:735–759. [PubMed: 10860799]

Miller, R. Cortico-Hippocampal Interplay and the Representation of Contexts in the Brain. Heidelberg: Springer-Verlag; 1991.

Miller R. Theory of the normal waking EEG: from single neurones to waveforms in the alpha, beta and gamma frequency ranges. Int J Psychophysiol 2007;64:18–23. [PubMed: 16997407]

Miwakeichi F, Martinez-Montes E, Valdes-Sosa PA, Nishiyama N, Mizuhara H, Yamaguchi Y. Decomposing EEG data into space-time-frequency components using Parallel Factor Analysis. Neuroimage 2004;22:1035–1045. [PubMed: 15219576]

Mizuhara H, Wang LQ, Kobayashi K, Yamaguchi Y. A long-range cortical network emerging with theta oscillation in a mental task. Neuroreport 2004;15:1233–1238. [PubMed: 15167540]

Moosmann M, Ritter P, Krastel I, Brink A, Thees S, Blankenburg F, Taskin B, Obrig H, Villringer A. Correlates of alpha rhythm in functional magnetic resonance imaging and near infrared spectroscopy. Neuroimage 2003;20:145–158. [PubMed: 14527577]

Mukamel R, Gelbard H, Arieli A, Hasson U, Fried I, Malach R. Coupling between neuronal firing, field potentials, and FMRI in human auditory cortex. Science 2005;309:951–954. [PubMed: 16081741]

Narayanan NS, Prabhakaran V, Bunge SA, Christoff K, Fine EM, Gabrieli JD. The role of the prefrontal cortex in the maintenance of verbal working memory: an event-related FMRI analysis. Neuropsychology 2005;19:223–232. [PubMed: 15769206]

Niessing J, Ebisch B, Schmidt KE, Niessing M, Singer W, Galuske RA. Hemodynamic signals correlate tightly with synchronized gamma oscillations. Science 2005;309:948–951. [PubMed: 16081740]

Nunez, PL.; Srinivasan, R. Electric Fields of the Brain: The Neurophysics of EEG. Oxford: Oxford University Press; 2006.

Onton J, Delorme A, Makeig S. Frontal midline EEG dynamics during working memory. Neuroimage 2005;27:341–356. [PubMed: 15927487]

Papademetris, X.; Jackowski, AP.; Schultz, RT.; Staib, LH.; Duncan, JS. Integrated intensity and point-feature non-rigid registration. In: Barillot, C.; Haynor, D.; Hellier, P., editors. Medical image computing and computer-assisted intervention. Saint_malo, France: Springer; 2004. p. 763-770.

Pascual-Marqui RD. Review of Methods for Solving the EEG Inverse Problem. International Journal of Bioelectromagnetism 1999;1:75–86.

Pascual-Marqui RD, Michel CM, Lehmann D. Low resolution electromagnetic tomography: a new method for localizing electrical activity in the brain. Int J Psychophysiol 1994;18:49–65. [PubMed: 7876038]

Percival, DB.; Walden, AT. Spectral Analysis for Physical Applications. Cambridge: Cambridge University Press; 1993.

Raichle ME, MacLeod AM, Snyder AZ, Powers WJ, Gusnard DA, Shulman GL. A default mode of brain function. Proc Natl Acad Sci U S A 2001;98:676–682. [PubMed: 11209064]

Rypma B, Prabhakaran V, Desmond JE, Glover GH, Gabrieli JD. Load-dependent roles of frontal brain regions in the maintenance of working memory. Neuroimage 1999;9:216–226. [PubMed: 9927550]

Sammer G, Blecker C, Gebhardt H, Bischoff M, Stark R, Morgen K, Vaitl D. Relationship between regional hemodynamic activity and simultaneously recorded EEG-theta associated with mental arithmetic-induced workload. Hum Brain Mapp. 2006

Sanchez-Arroyos R, Gaztelu JM, Zaplana J, Dajas F, Garcia-Austt E. Hippocampal and entorhinal glucose metabolism in relation to cholinergic theta rhythm. Brain Res Bull 1993;32:171–178. [PubMed: 8348341]

Schack B, Klimesch W. Frequency characteristics of evoked and oscillatory electroencephalic activity in a human memory scanning task. Neurosci Lett 2002;331:107–110. [PubMed: 12361852]

Schack B, Vath N, Petsche H, Geissler HG, Moller E. Phase-coupling of theta-gamma EEG rhythms during short-term memory processing. Int J Psychophysiol 2002;44:143–163. [PubMed: 11909647]

Sederberg PB, Kahana MJ, Howard MW, Donner EJ, Madsen JR. Theta and gamma oscillations during encoding predict subsequent recall. J Neurosci 2003;23:10809–10814. [PubMed: 14645473]

Shmuel A, Yacoub E, Pfeuffer J, Van de Moortele PF, Adriany G, Hu X, Ugurbil K. Sustained negative BOLD, blood flow and oxygen consumption response and its coupling to the positive response in the human brain. Neuron 2002;36:1195–1210. [PubMed: 12495632]

Siapas AG, Lubenov EV, Wilson MA. Prefrontal phase locking to hippocampal theta oscillations. Neuron 2005;46:141–151. [PubMed: 15820700]

Stefanovic B, Warnking JM, Pike GB. Hemodynamic and metabolic responses to neuronal inhibition. Neuroimage 2004;22:771–778. [PubMed: 15193606]

Sternberg S. High-speed scanning in human memory. Science 1966;153:652–654. [PubMed: 5939936]

Thomson, DJ.; Chave, AD. Jackknifed error estimates for spectra, coherences, and transfer functions. In: Haykin, S., editor. Advances in Spectrum Analysis and Array Processing. Prentice Hall: 1990.

Tsujimoto T, Shimazu H, Isomura Y. Direct recording of theta oscillations in primate prefrontal and anterior cingulate cortices. J Neurophysiol. 2006

Tuladhar AM, Huurne NT, Schoffelen JM, Maris E, Oostenveld R, Jensen O. Parieto-occipital sources account for the increase in alpha activity with working memory load. Hum Brain Mapp 2007;31:31.

Uecker A, Barnes CA, McNaughton BL, Reiman EM. Hippocampal glycogen metabolism, EEG, and behavior. Behav Neurosci 1997;111:283–291. [PubMed: 9106669]

Van Winsum W, Sergeant J, Geuze R. The functional significance of event-related desynchronization of alpha rhythm in attentional and activating tasks. Electroencephalogr Clin Neurophysiol 1984;58:519–524. [PubMed: 6209102]

Vanni S, Revonsuo A, Hari R. Modulation of the parieto-occipital alpha rhythm during object detection. J Neurosci 1997;17:7141–7147. [PubMed: 9278548]

Wei X, Yoo SS, Dickey CC, Zou KH, Guttmann CR, Panych LP. Functional MRI of auditory verbal working memory: long-term reproducibility analysis. Neuroimage 2004;21:1000–1008. [PubMed: 15006667]

Winterer G, Carver FW, Musso F, Mattay V, Weinberger DR, Coppola R. Complex relationship between BOLD signal and synchronization/desynchronization of human brain MEG oscillations. Hum Brain Mapp. 2006

Yamagishi N, Callan DE, Goda N, Anderson SJ, Yoshida Y, Kawato M. Attentional modulation of oscillatory activity in human visual cortex. Neuroimage 2003;20:98–113. [PubMed: 14527573]

Zarahn E, Rakitin B, Abela D, Flynn J, Stern Y. Positive evidence against human hippocampal involvement in working memory maintenance of familiar stimuli. Cereb Cortex 2005;15:303–316. [PubMed: 15342440]

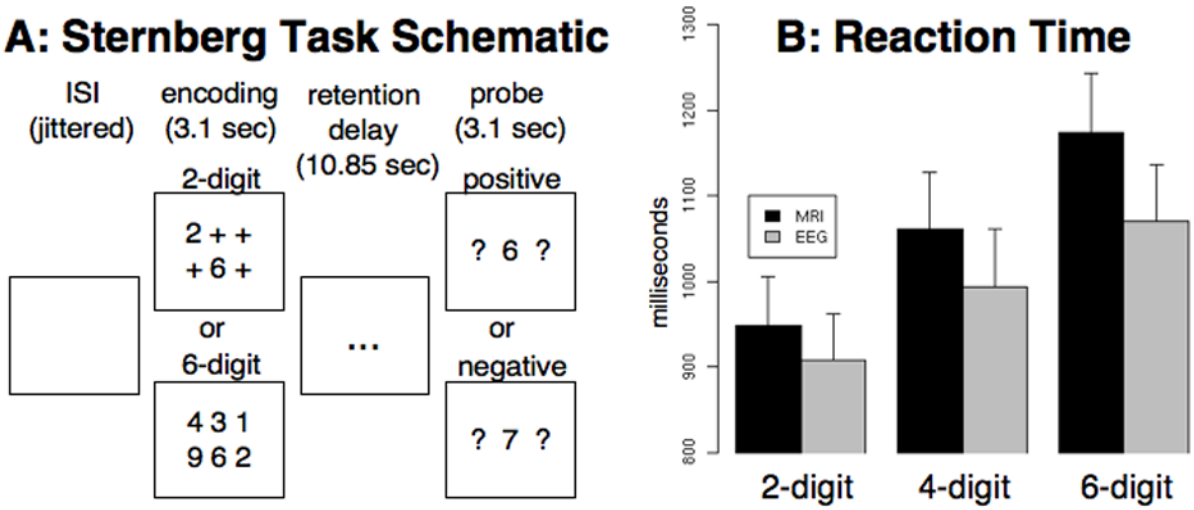


**Fig. 1. The Sternberg task**

A: Schematic of the trial design. The 4-digit condition is not shown.

B: Average reaction times for the three levels of working memory load in the two sessions, fMRI and EEG. Error bars represent standard error of the mean.

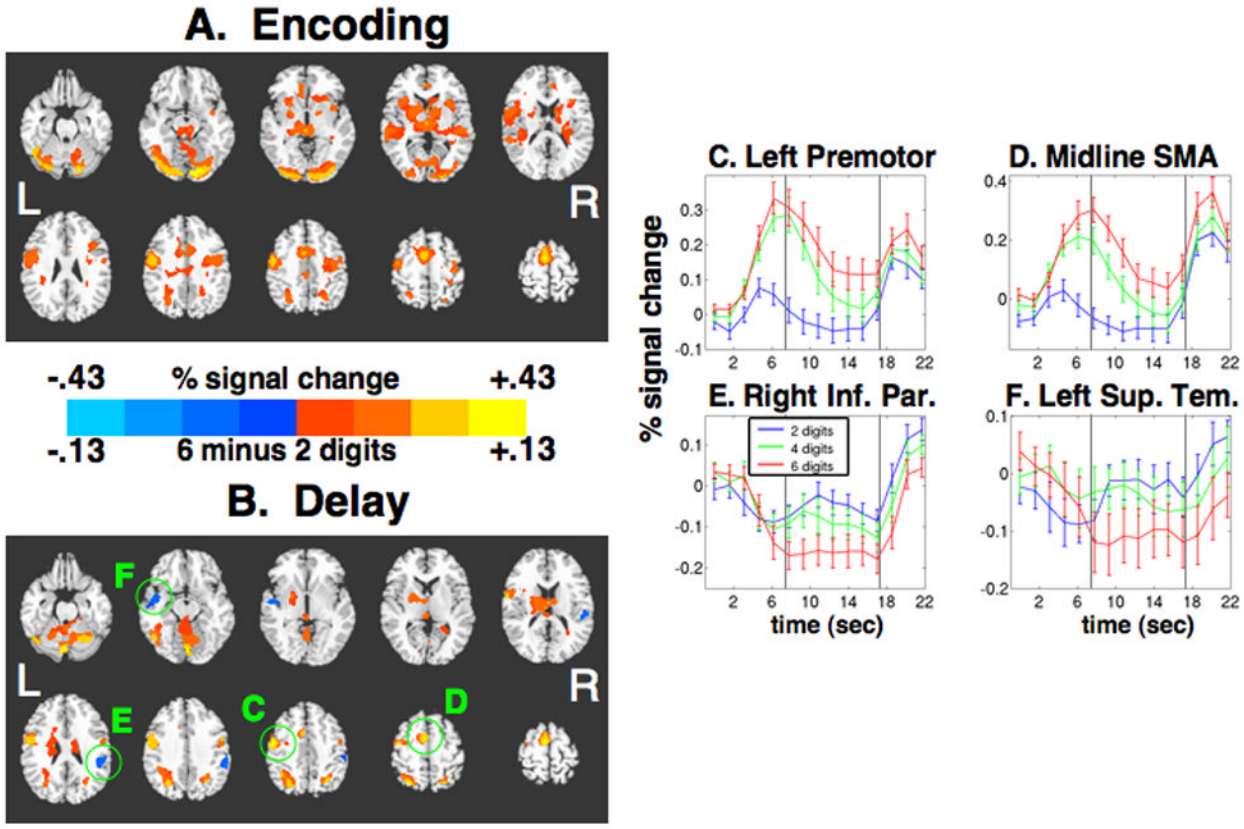


**Fig. 2. FMRI of the Sternberg task**

A: Load-dependent activity during encoding, 6 digits minus 2 digits. Voxel-wise threshold of p<.005, p<.05 corrected. Extensive prefrontal and inferior parietal activation is seen, as in previous studies of the Sternberg task. No deactivations were found.

B: Load-dependent activity during the delay period of the Sternberg task, 6-digits minus 2-digits, thresholding identical to panel A. Activation is seen in many similar areas as during encoding, although load-dependent decreases are also present.

C–F: Averaged BOLD timecourse in a functionally identified ROIs in left premotor cortex, supplementary motor area (positively modulated by memory load), and in right inferior parietal cortex, and left superior temporal cortex (negatively modulated). Delay period activity is indicated by vertical bars (see text). These four areas are circled within figure 2B. Error bars represent standard error of the mean for each timepoint.

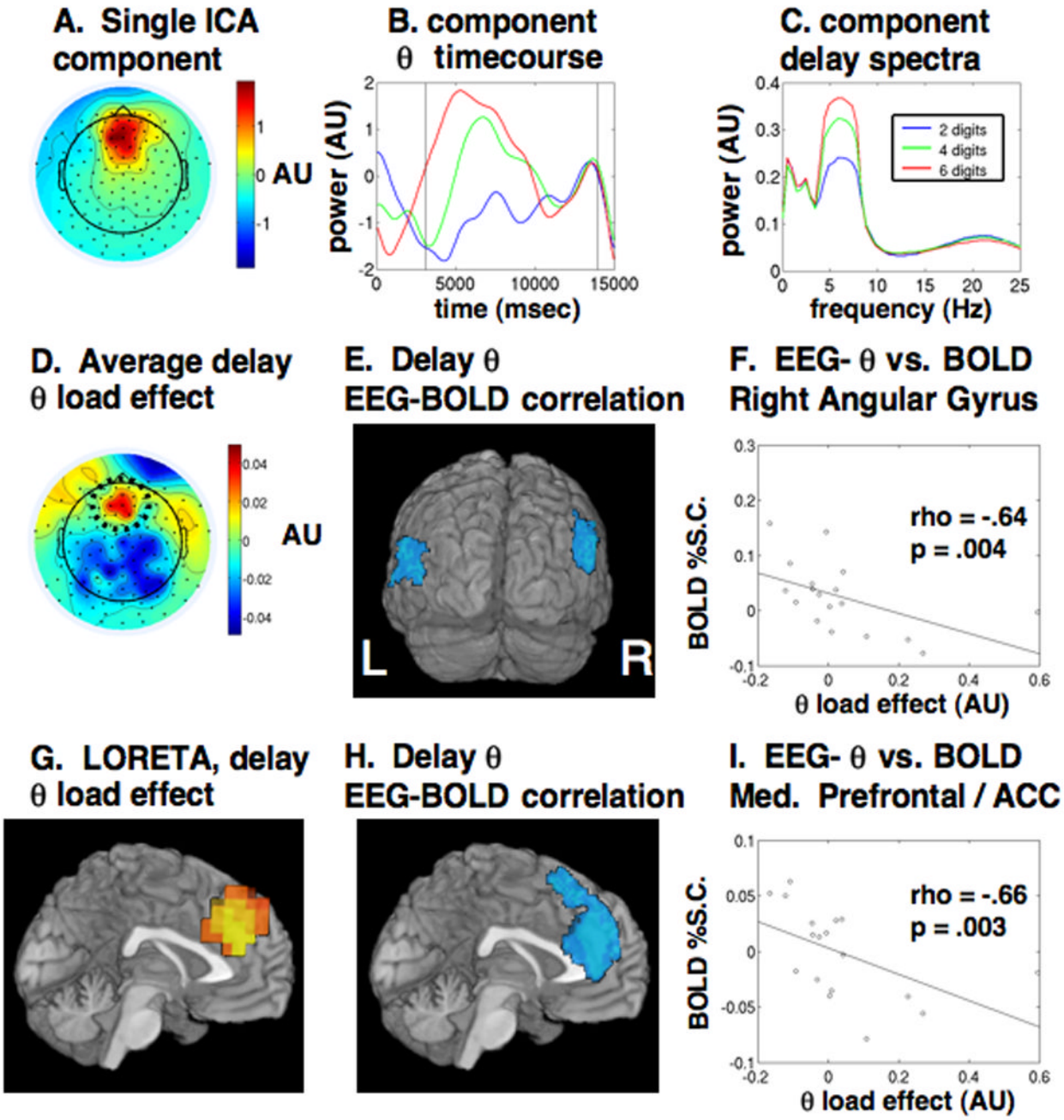


**Figure 3. Theta power dynamics and relationship with BOLD**

Note: Figure panels are organized to facilitate relevant visual comparisons and do not exactly match the order in which they are discussed in the text.

A: ICA component scalp distribution for a component dominated by reactive theta activity, in a subject showing a clear theta power increase with memory load. The values represent the degree to which the component contributes to the signal at each electrode.

B: Timecourse of theta power for the component shown in panel B, showing the load-dependent increase specific to the delay period.

C: Delay period power spectra for the example theta component.

D. Group average topographic map of load effect (6-digit minus 2-digit) for delay period theta power. The black ellipse is the region of interest used for computation of EEG-BOLD correlations. Values represent power from 4–7 Hz subtracted between the two conditions, divided by the total average power in all conditions from 0–30 Hz (in each subject), and then averaged across subjects.
E: Posterior view of regions showing across-subjects correlation between frontal theta power and BOLD load effects.
F: Theta power vs. BOLD load effects in the right angular gyrus.
G: LORETA source localization of theta power load effect, averaged across all subjects and thresholded statistically at $p<.01$ voxel-wise.
H: Midline view of regions showing across-subjects correlation between delay period frontal theta power and BOLD load effects.
I: Theta power vs. BOLD load effects in the medial prefrontal cortex.

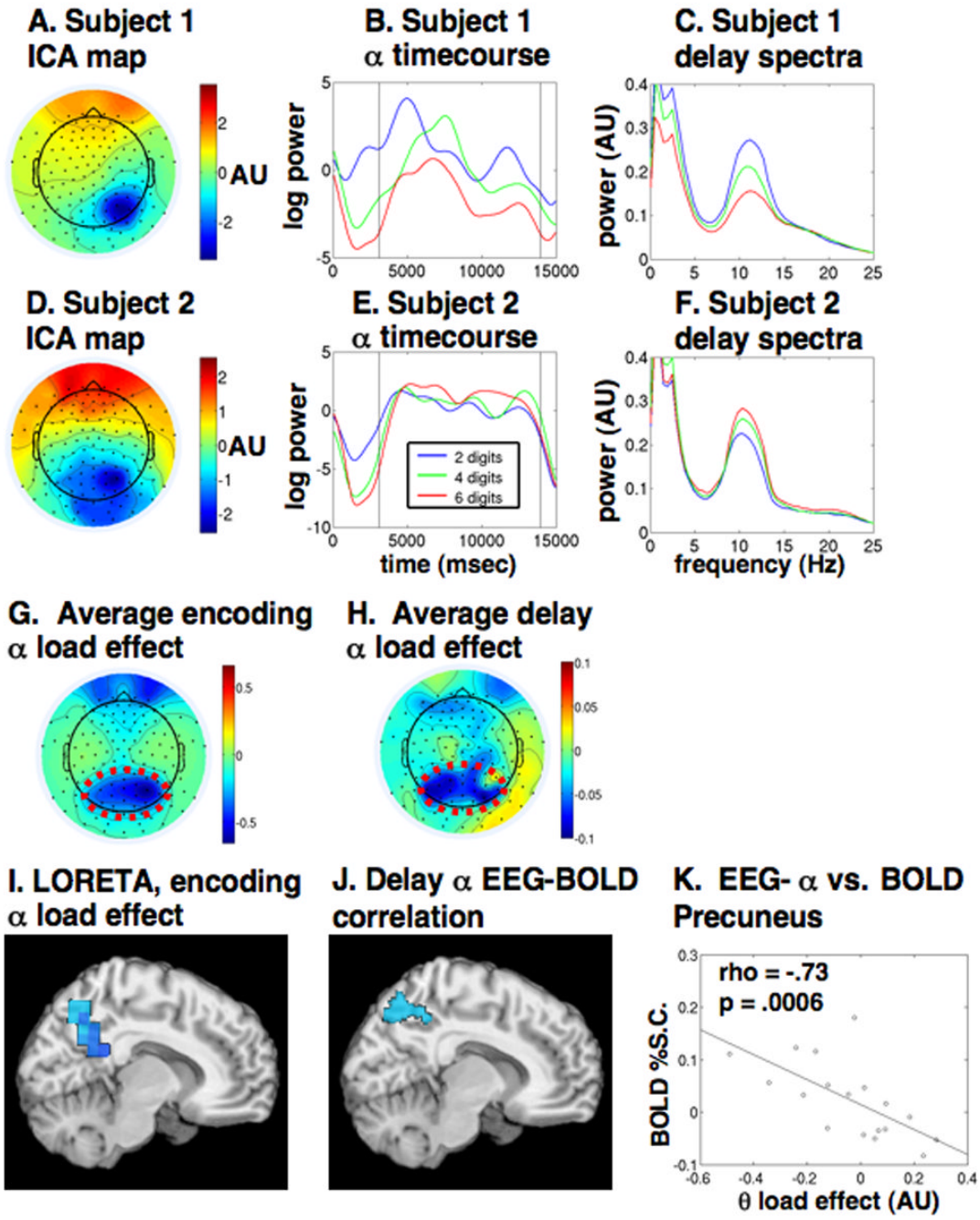


**Fig. 4. Alpha power dynamics and relationship with BOLD**

Note: Figure panels are organized to facilitate relevant visual comparisons and do not exactly match the order in which they are discussed in the text.

A: Group average scalp map of alpha power difference (6 digits minus 2 digits) during the encoding period (0–3 seconds after digit array presentation). Values computed as in figure 3D.

B: Group average power spectra in the posterior scalp ROI (indicated by the ellipse in panel A), demonstrating load-dependent alpha power suppression. Values computed as in figure 3D.

A: ICA topographic map from one subject (Subject 1), showing the scalp distribution of a posterior alpha rhythm component. Values computed as in figure 3A.

B: Timecourse of alpha power for the alpha component in Subject 1, showing a load-dependent decrease during the encoding period (0–3.10 seconds), followed by a sustained load-dependent suppression throughout the delay period (3.10–13.95 seconds).
C: Power spectra during the delay period for the alpha of Subject 1, showing a load-dependent suppression of alpha power.
D. ICA topographic map from a second subject (Subject 2), showing the scalp distribution of a posterior alpha rhythm component. Values computed as in figure 3A.
E: Timecourse of alpha power for the alpha component in Subject 2, showing a load-dependent alpha power *decrease* during the encoding period, followed by load-dependent power *increase* during the delay period.
F: Power spectra during the delay period for the alpha component of Subject 2, showing a load-dependent increase of alpha power.
G. Group average topographic map of load effect (6-digit minus 2-digit) for encoding period alpha power. The black ellipse is the region of interest used for computation of EEG-BOLD correlations.
H. Group average topographic map of load effect for delay period alpha power. The black ellipse is the region of interest used for computation of EEG-BOLD correlations.
I: LORETA source localization of the alpha power load effect during the encoding period, averaged across subjects and thresholded statistically at $p<.01$ voxelwise.
J: Midline view of regions showing across-subjects correlation between delay period posterior alpha power and BOLD load effects.
K: Alpha power vs. BOLD load effects in the precuneus.

**Table 1**

Table 1A. Encoding 6 Digits Minus 2 Digits.
Table 1B. Delay Retention, 6 Digits Minus 2 Digits
Table 1C. Rank Order Correlation Between Load-Dependent Theta Power And BOLD
Table 1D. Rank Order Correlation Between Load-Dependent Alpha Power And BOLD

| Label | Volume* | Max. Intensity** | X† | Y† | Z† |
|---|---|---|---|---|---|
| L Ant. Precentral, Inf. Frontal, Sup. Temporal Gyri, Bilat. Striatum | 5924 | 0.3315 | −33.3 | −9.5 | 17.7 |
| R Lingual/Fusiform Gyri | 2492 | 0.4263 | 19.9 | −84.5 | −7.6 |
| L Lingual/Fusiform Gyri | 2034 | 0.3673 | −30.6 | −80.5 | −12.2 |
| Dorsal Medial Prefrontal Gyrus | 1883 | 0.3881 | −4.1 | 4.8 | 56.7 |
| R Anterior Precentral Gyrus | 1173 | 0.209 | 39.7 | −6 | 41.4 |
| R Superior Temporal Gyrus | 629 | 0.1245 | 37.8 | −29.1 | 10.2 |
| L Inferior Parietal Lobe | 527 | 0.2214 | −28.3 | −57.3 | 44.9 |
| R Inferior Frontal Gyrus | 298 | 0.1558 | 36.6 | 14.8 | 13.9 |
| R Inferior Parietal Lobe | 276 | 0.1707 | 23.9 | −54.9 | 46.3 |

| Label | Volume* | Max. Intensity** | X† | Y† | Z† |
|---|---|---|---|---|---|
| Medial Cerebellum | 3232 | 0.1228 | 7.8 | −62.6 | −26 |
| Bilateral Caudate/L Putamen | 1368 | 0.0733 | −12.3 | −7.7 | 15 |
| L Inferior Parietal Lobe | 1184 | 0.1033 | −29.4 | −58.2 | 44.6 |
| L Anterior Precentral Gyrus | 964 | 0.1288 | −52.4 | −1.7 | 36.5 |
| Dorsal Medial Prefrontal Gyrus | 646 | 0.1302 | −6.5 | 2.6 | 61.8 |
| R Inferior Parietal Lobe (negative) | 460 | −0.0664 | 54 | −31.7 | 30 |
| L Fusiform Gyrus | 395 | 0.0944 | −45.7 | −60.5 | −17.9 |
| L Insula (negative) | 247 | −0.0495 | −50 | −6.4 | −8.7 |
| R Anterior Precentral Gyrus | 210 | 0.079 | 52.2 | −2.2 | 35.8 |
| R Posterior Parahippocampal Gyrus | 209 | 0.0693 | 26.7 | −56 | 21.4 |

| Label | Volume* | Max. Intensity** | X† | Y† | Z† |
|---|---|---|---|---|---|
| Med. Preftl. Ctx./Ant. Cingulate | 4872 | −.88 | −2 | 34 | 33 |
| R Angular Gyrus/Lateral Parietal | 582 | −.82 | 51 | −61 | 27 |
| L Angular Gyrus/Lateral Parietal | 214 | −.80 | −58 | −48 | 12 |
| Left Middle Frontal Gyrus | 297 | −.89 | −41 | 19 | 46 |

| Label | Volume* | Max. Intensity** | X† | Y† | Z† |
|---|---|---|---|---|---|
| Precuneus | 281 | −.77 | −7 | −63 | 47 |

*Volume given in voxels. Voxel size is 2×2×2 mm.

**Intensity values are average regression parameter estimates across subjects. Units are essentially arbitrary.

*** Intensity values are Spearman's Rho rank-order correlation coefficient.

† Spatial coordinates are mm in MNI space.